[Title]

Real-time assessment of surface interactions with titanium passivation layer by surface plasmon resonance

[Author List]

Isao Hirata [a,*], Yasuhiro Yoshida [b], Noriyuki Nagaoka [b], Kyou Hiasa [a], Yasuhiko Abe [a], Kenji Maekawa [b], Takuo Kuboki [b], Yasumasa Akagawa [a], Kazuomi Suzuki [b], Bart Van Meerbeek [c], Phillip B. Messersmith [d], Masayuki Okazaki [a]

[a] Graduate School of Biomedical Sciences, Hiroshima University, 1-2-3 Kasumi, Minami-ku, Hiroshima 734-8553, Japan

[b] Graduate School of Medicine, Dentistry and Pharmaceutical Sciences, Okayama University, 2-5-1 Shikata-cho, Kita-ku, Okayama 700-8525, Japan

[c] Leuven BIOMAT Research Cluster, Department of Conservative Dentistry, Catholic University of Leuven, Kapucijnenvoer 7, B-3000 Leuven, Belgium

[d] Department of Biomedical Engineering, Northwestern University, 2145 Sheridan Road, Evanston, Illinois 60208, USA

* Corresponding author. Fax: +81-82-257-5649.

E-mail address: isao@hiroshima-u.ac.jp (I. Hirata).

[Abstract]

The high corrosion resistance and strength-to-density ratio makes titanium widely used in major industry, but also in a gamut of medical applications. Here we report for the first time on our development of a titanium passivation layer sensor that makes use of surface plasmon resonance (SPR). The deposited titanium metal layer on the sensor was passivated in air, like titanium medical devices. Our ‘Ti-SPR sensor’ enables analysis of biomolecules interactions with the passivated surface of titanium in real time. As a proof of concept, corrosion of titanium passivation layer exposed to acid was monitored in real time. Also, the Ti-SPR sensor can accurately measure the time-dependence of protein adsorption onto titanium passivation layer with a sub-nanogram per square millimeter accuracy. Besides such SPR analyses, an SPR-imaging (SPRI) enables real-time assessment of chemical surface processes that occur simultaneously at ‘multiple independent spots’ on the Ti-SPR sensor, such as acid-corrosion or adhesion of cells. Our Ti-SPR sensor will therefore be very useful to study titanium-corrosion phenomena and biomolecular titanium-surface interactions with application in a broad range of industrial and biomedical fields.

[Keywords]

Titanium passivation layer; Surface plasmon resonance; Protein adsorption; Cell adhesion; Biosensor

[Text]

1. Introduction

Thanks to high strength-to-density, excellent corrosion resistance decreasing cost and increasing availability, titanium and its alloys enjoy their widespread industrial applications in a wide variety of highly corrosive environments including sea water, bleaches, alkaline solutions, oxidizing and organic acids [1]. These excellent properties make titanium widely used in industries including aerospace, marine, power generation, and desalination plants for instance [2-5]. Their extremely high corrosion resistance results from the formation of a very stable, continuous, highly adherent, and protective oxide film on the titanium surface, formed spontaneously and instantly once fresh metal surfaces are exposed to air, or moisture.

Titanium is also commonly used to fabricate a variety of medical devices such as hip and knee joints, bone screws and plates, dental implants, stents, pacemaker cases and centrifugal pumps of artificial hearts [6-8]. Due to the rapidly ageing population, especially in developed countries, the national health care costs are escalating. In particular, the increased incidence of hard tissue and cardiovascular diseases such as periodontitis, osteoarthritis, and arteriostenosis is strongly correlated with the rapidly growing elderly population. Therefore, the development of innovative treatment techniques for functional repair or complete cure of these diseases is highly desirable. In attempts to improve the healing potential of such medical devices, much research is devoted to titanium-surface modification methods that enable controlled adsorption of biomolecules and ions, or regulated drug release [9-12]. In biomaterial sciences,

the strategic importance of fundamental research in nano-biotechnology has recently been acknowledged [13]. The developments of highly sensitive methods that can monitor the interaction of biomolecules at titanium surfaces are therefore highly needed.

Surface plasmon resonance (SPR) can offer real-time and label-free analysis of the interfacial events that occur on the surface of a metal layer under physiological conditions [14-15]. Recently, the technique of SPR imaging (SPRI) has been developed and applied to monitor the adsorbing organic materials and biomolecules at multiple independent spots [16]. In this study, we report for the first time on our development of a titanium passivation surface sensor chip for SPR [17]. There are few reports of the titanium SPR (Ti-SPR) sensor which titanium metal layer was passivated in air. Although many studies of a TiO_2-coated sensor for SPR are reported [18-23], their sensors were coated by TiO_2 directly and titanium metal was not used. In medicine and dentistry, the titanium metal surface of dental implants and artificial bones oxidize in air. Our Ti-SPR sensor has the titanium passivation layer, closely resembling the condition under which titanium medical devices are normally used during clinical treatment.

2. Experimental section

2.1 Materials

Bovine serum albumin was purchased from Sigma-Aldrich Japan K.K. (Tokyo, Japan). γ-Globulin was purchased from Nacalai Tesque, Inc. (Kyoto, Japan). bFGF (recombinant human basic growth factor: KCB-1) was kindly donated by

KAKEN Pharmaceutical CO., Ltd. (Kyoto, Japan). Dulbecco's phosphate buffered saline without calcium and magnesium (PBS; pH 7.4) was purchased from Nissui Pharmaceutial Co., Ltd. (Tokyo, Japan). Dodecylphosphate (DDP) was purchased from Alfa Aesar (Ward Hill, MA). Other chemicals were purchased from Wako Pure Chemical Industries (Osaka, Japan). All chemicals were used as received without any additional purification. Glass Plates made of S-LAL10 (refractive index: 1.72; diameter: 15 mm, thickness: 1 mm) were purchased from Arteglass Associates Co. (Kyoto, Japan).

2.2 Surface Plasmon Resonance Instruments

We constructed a surface plasmon resonance (SPR) instrument which observes an SPR spectrum and an SPR angle shift [24-25]. The SPR instrument, constructed by referring to Knoll's method, utilized the Kretschmann configuration in which a metal was in the form of a thin film mounted directly onto a S-LAL10 glass plate coupled to an S-LAL10 dispersing prism with an index matching fluid [14, 26]. An SPR chip was set on the SPR flow cell, which was 10 mm in length, 1 mm in width, and 1 mm in thickness. Solutions were allowed to pass through the flow cell [25]. The He-Ne laser light (λ; 632.8 nm) was linearly *p*-polarized using a Gran-Thomson prism and then passed through a non-polarizing cube beam-splitter. The sample surface was exposed to the *p*-polarized light through the prism. The intensity of the reflected light was determined by a photo diode detector. A computer was used to control a biaxial rotation stage and to process the intensities of the incident and the reflected light as a SPR spectrum. At an angle of a dip of the spectrum, the light was resonated

surface plasmons on the metal layer and this angle is called as an SPR angle. [14-15]

The SPR imaging (SPRI) apparatus employed in this study was used SPR-1000 (UBM, Kyoto, Japan), which was developed by referring our constructed SPRI [16]. The SPR chip with arrayed spots was mounted on an S-LAL10 dispersing prism with index matching fluid. The flow cell was constructed using a washer made of silicone and a vinyl chloride lid with an inlet and outlet. The back side of the chip was illuminated by a *p*-polarized, collimated, and polychromatic white light through the prism. The reflected light was passed through an interference filter and collected by a CCD camera. The data was acquired by our designed software.

The Ti-SPR sensor chip can be used in both instruments. All experiments were carried out at 25 °C.

2.3 Development and Evaluation of Titanium SPR Sensor

2.3.1 Design of Titanium SPR sensor

General SPR sensor chips are based on gold coated glass substrate. The Ti-SPR sensor chips were prepared by depositing titanium metal on a contamination-free gold surface of the SPR sensor. For designing of an optimal Ti-SPR sensor, it was necessary to consider the thickness and oxidation of the deposited titanium layer and detection of protein adsorptions in water solutions. So, the SPR spectra of the Ti-SPR sensor were simulated by the Fresnel equation of reflection and transmission using prism, glass plate, Cr, Au, Ti, TiO_2, protein, and water multilayer (Fig. 1) for estimation of an optimal layer thickness

of the deposited titanium [26-27]. When an amount of proteins adsorption or a thickness of TiO_2 layer is changed, the SPR angle is shifted. So, the shift of the SPR angle (degree) can be calculated as the amount of proteins (4.02 ng•mm^{-2}•degree^{-1}) or the thickness of the etched TiO_2 layer (0.77 nm •degree^{-1}).

The designed Ti-SPR sensor chips were prepared by Osaka Vacuum Industrial Co. Ltd. (Osaka, Japan). These chips were prepared by depositing Cr, Au, and Ti on the S-LAL10 glass plates under 2.0×10^{-2} Pa using an electron-beam evaporation method.

2.3.2 Characterization of Titanium Layer on Ti-SPR sensor

A transmission electron microscopy (TEM) cross-section of the developed Ti-SPR sensor chip embedded in epoxy resin was prepared using an Ion Slicer (EM-09100IS, JEOL), and imaged using a JEM-3010 (JEOL) TEM operated at 300kV. The surface elemental composition of the Ti-SPR sensor was determined using an X-ray photoelectron spectroscopy (XPS; AXIS-HS, Kratos, Manchester, UK) *in vacuo* at less than 10^{-7} Pa. We used Al-Kα monochromatic x-ray with a source power of 150 W (acceleration voltage of 15 kV and filament current of 10 mA) and measured the elemental composition ratio of Au, Ti, and O at photo-electron take-off angles of 90, 60, 45, 30, and 15 degrees. The layer thicknesses of the titanium and the oxidized titanium on the Ti-SPR sensor were estimated by the SPR spectrum of this sensor and the relationship between the proteins amount of adsorbed and the SPR angle shift was determined.

2.4 SPR Measurements of Acid Etching and Biomolecule Adsorption

2.4.1 Effect of Acid Etching on Titanium Surface

The effect of acid etching of titanium surface was determined by SPR. Phosphoric-acid solutions were prepared by dropping 85 wt% phosphoric acid into pure water until these pH were 1.8, 1.9, 2.0, and 3.0, respectively and the running solution used was pure water. The Ti-SPR sensor chip was set on an SPR flow cell. Pure water was allowed to pass through the flow cell until the SPR angle was stable. The SPR spectrum was recorded for the Ti-SPR sensor exposed to pure water and then the incident light angle was fixed at 1.0 degree lower than the minimum of the reflectance, which was the SPR angle. Subsequently, the intensity of the reflected light was followed during exposed to the phosphoric acid solution under flow for 20 min. Then, this solution was washed out with the water for 19 min and the SPR spectrum was recorded again. The SPR angle shift was determined from the minima of the two resonance profiles.

The effect of acid etching of titanium was also determined by Quartz Crystal Micro-balance (QCM, Q-Sense D300). A QSX 310 (titanium QCM sensor) was attached to a QCM flow cell (QWiC301). All QCM apparatuses and chips were purchased from Q-Sense AB (Västra Frölunda, Sweden). Pure water was allowed to pass through the flow cell until a frequency of the quartz crystal was stable. Subsequently, the phosphoric-acid solution was allowed to flow for 20 min. Finally, this solution was washed out of the flow cell with pure water for 19 min. The phosphoric-acid solutions used had either pH of 1.8 or 2.0.

All solutions were flowed at 3.3 ml/min in both experiments.

2.4.2 Protein and Polymer Adsorption on Titanium Surface

The amount of protein and polymer adsorbed onto the titanium surface was determined by the Ti-SPR sensor. The Ti-SPR sensor chip was set on the SPR flow cell and then PBS was allowed to pass through the flow cell at 3.3 ml/min. After the SPR angle was stable, the SPR spectrum was recorded. Subsequently, the intensity of the reflected light was followed during exposure to a protein or polymer solution under flow for 10 min. Then, this solution was washed out with PBS for 9 min and the SPR spectrum was recorded again. The protein solutions used were 2 μg/ml albumin, γ-globulin, and bFGF in PBS. The polymer solutions used were 100 μg/ml polyethyleneimine (PEI) and gelatin in PBS, and 1 wt% poly phosphoric acid (PPAc) in water.

2.5 SPRI Measurements of Cell Response and Corrosion Resistance

2.5.1 Preparation of Titanium Array for SPRI

The titanium surface of the Ti-SPR sensor chip was cleaned by argon-plasma irradiation (electrode current of 23 mA for 90 seconds), and then immersed in acetone and toluene for 5 minutes each. This washed chip was then immersed in 2 mM octadecyltrichlorosilane (ODTCS) dissolved into toluene for 24 hours at 60ºC. After silane-treatment, this chip was washed successively with toluene, acetone, a 1:1 (v/v) acetone-water mixture, and finally again with acetone. This OTDCS layer adsorbed onto the titanium surface was then irradiated/etched with argon plasma (electrode current of 10 mA for 10 minutes), after having positioned a stainless steel mask pattern (5x5 pore arrays with a circular pore size of 1 mm, and an inter-pore space of 1 mm) in order to make 1 mm diameter

titanium spots on the OTDCS-coated Ti-SPR sensor chip. This patterned array chip was immersed in acetone.

2.5.2 Preparation of Polymer-Coated Titanium Array

The polymer-coated titanium array chip was prepared by dropping 1 µl PBS onto the titanium spots of the titanium array chip, after which the chip was kept in saturated water vapor for 20 minutes. Then, the PBS drops were removed and 0.5 µl of PEI, gelatin, PPAc, and PBS were dropped onto these spots, after which the chip was again kept in saturated water vapor for 20 minutes. Finally, each spot was 5 times washed with PBS.

2.5.3 Interaction of cells with titanium assessed using SPRI

The interaction of cells onto the polymer-coated titanium array chip was determined by SPRI. An albumin free PIPES-buffered medium (25 mM PIPES (pH 7.2), 159 mM NaCl, 5 mM KCl, 0.4 mM $MgCl_2$, 1 mM $CaCl_2$, 5.6 mM glucose) [28] was prepared as solvent and the sample solution used was a MC3T3-E1 cell suspension (500,000 cells in 1 ml of this medium). The chip was attached to an SPRI batch cell. 300 µl of the medium was dropped onto the batch cell and the SPRI image was allowed to stabilize. Then, 100 µl of the cell suspension was dropped onto the batch cell and mixed in situ, while the SPRI image data was recorded for 1 hour. Under the above-mentioned condition, phase contrast microscopy images of cell attachment on the polymer-spotted array chip were made.

2.5.4 Preparation of DDP treated Titanium Array

The DDP treated array chip was prepared by dropping 0.3 μl of 1wt% DDP dissolved in 1:1 (wt/wt) water-ethanol mixture onto the titanium spots of the titanium array chip, after which the chip was kept in saturated water vapor for 30 minutes. Then, the chip was washed with acetone 3 times.

2.5.5 Observation of Corrosion Resistance of DDP treated Titanium by SPRI

The process of acid etching onto the DDP coated titanium array chip was observed by the SPRI for 10 min. An HCl/KCl-buffered solution (pH 1.5; 41.4 mM HCl and 50.0 mM KCl) [29] and a KCl solution (63.1 mM KCl) were prepared as the 'running' and the 'sample' solution, respectively. The chip was attached to an SPRI flow cell. The running solution was allowed to pass through the flow cell and the SPRI image was allowed to stabilize. Then the SPRI data was recorded simultaneously at the different spots during exposure to the sample solution at a flow rate of 3.3 ml/min.

3. Results and discussion

3.1 Development of Titanium SPR Sensor

For the design of the Ti-SPR sensor, the SPR spectrum needed to be simulated. Figure 2 shows the simulated SPR spectra in relation to the thickness and the oxidation rates of the titanium layers. The titanium layer deposited on the SPR sensor chip easily oxidizes in air (leading to increased corrosion-resistance). When the titanium layer (atomic weight; 47.9, density; 4.5 g/cm^3) is oxidized to the titanium dioxide layer (molecular weight; 79.9), its

density is reduced and its thickness is increase [30]. A density of titanium dioxide crystal is 3.8 g/cm^3 (antase) or 4.2 g/cm^3 (rutile) and the oxidized titanium layer on the Ti-SPR sensor was expected to be low crystallinity and to be contained many hydroxyl groups [30-32], we assumed that the density of the oxidized titanium layer was 4.0 g/cm^3 and its layer grew in the uni-axial direction and the thickness of this layer increased 1.9 times as a result of oxidization. In the case of a 5 nm thick of titanium surface layer, the peak of the SPR spectrum was sharpened with the degree of oxidation. In case of a 10 nm titanium layer, however, the peak of the SPR spectrum did not sharpen and the SPR angle, which is a minimum reflectance angle in the SPR spectrum, occurred at high incident light angle. The latter is disadvantageous because the amount of protein adsorption is related to the increase of the SPR angle. In case of a 20 nm Ti layer, the peak of the SPR spectrum did not occur. These simulations suggest that the thinner the titanium layer is, the more accurate ('sharper') the SPR spectrum is. Therefore, a Ti-SPR sensor with the most optimal 5 nm thick metal titanium layer was employed.

3.2 Evaluation of Ti-SPR sensor Surface

The simulation was not sufficient to determine the actual thickness of surface oxide layer. So we measured the Ti-SPR sensor chip, as shown in figure 3 and 4 using TEM and SPR. The thinnest achievable titanium layer that could be sputter-coated was 5 nm. High-magnification cross-sectional TEM image of the Ti-SPR sensor (fig. 3) showed the 49 nm Au layer with about 10 nm Ti/TiO_2 layer on top and the Cr-layer underneath on top of the glass substrate. In the SPR

result (fig. 4), the spectrum of the Ti-SPR sensor was detected and the thickness of the oxide layer was obtained by comparing both the simulated and the measured SPR spectra. The dotted line in the figure shows the simulated SPR spectrum for a 0.7 nm thick titanium layer and a 7.6 nm titanium dioxide layer. Good agreement was found for the actual and simulated SPR spectra.

Figure 5 shows the results of the atom fraction of Au and the O/Ti ratio at the Ti-SPR sensor surface as measured by angle-dependent XPS, confirming that the gold layer was uniformly coated with an ultrathin oxidized titanium layer, and that the O/Ti ratio at the top was larger than at the bottom. The nonstoichiometric O/Ti ratio may be due to the fact that the outer surface contained titanium hydroxide ($TiO(OH)_2$ with an O/Ti ratio of 3, while the O/Ti ratio of TiO_2 is 2), and because oxygen of these hydroxyl groups seemed to mainly exist at the top layer. From these results, the external layer of the titanium surface SPR sensor was concluded to be the titania.

3.3 Detection of Acid Etching on Titanium Surface

Titanium is very corrosion-resistant thanks to the presence of the passivating film on the surface. When we exposed the surface of the Ti-SPR sensor to phosphoric-acid solutions with different pH (fig. 6a), the SPR angles shifted to a lower angle except for the pH=3.0 solution. This indicates that the oxidized titanium surface was etched when exposed to phosphoric-acid solutions with a pH of 2.0 or below. The average thickness changes at pH 2.0, 1.9, and1.8 were about 20 pm, 50 pm, and 120 pm, respectively.

Using QCM, the effect of etching titanium was also determined under the

same conditions (fig. 6b), but the relatively low signal-to-noise ratio obscured the QCM spectrum. Pressure fluctuation of the flowing solution strongly affects the frequency of the quartz crystal, whereas the optical performance of the Ti-SPR sensor is largely unaffected under similar conditions. For measuring titanium etching, the Ti-SPR sensor has a high-sensitivity, which is achieved because TiO_2 has a higher dielectric constant (ε: 5.19) than phosphoric acid (ε: 2.12) [33] in water, and consequently the SPR angle shift due to changes in layer thickness is about 5 times more sensitive for TiO_2 (0.77 nm•degree^{-1}) than for phosphoric acid (4 nm•degree^{-1}).

The above-mentioned experiments confirm the real-time high-resolution acid-etching measuring capability of the Ti-SPR sensor.

3.4 Measurement of Biomolecule adsorption on Titanium Surface

Thanks to high biocompatibility, titanium is commonly used a variety of medical devices. However, chemical and biological reactions of non-treated titanium surface are poor because of its chemical stability. Therefore many modification methods of titanium surface have been studied for increasing bioactivity, bone conductivity, and biocompatibility. [32, 34-35]

In this study, the Ti-SPR sensor was used to measure the interaction between biomolecules and titanium passivation layer in real time. Figure 7 shows the increasing protein absorption on Ti with time for the three proteins studied. It was assumed that the difference in pI and molecular weight of the proteins would influence absorbed the protein amounts. At pH 7.4, the Ti surface is negatively charged [36], γ-globulin is slightly negatively charged, albumin is negatively

charged, and bFGF is positively charged. Therefore, we consider that γ-globulin (158 kDa, pI 5.8-7.3) was most adsorbed on Ti (2.85 ng/mm^2) because of its largest molecular weight, albumin (69 kDa, pI 4.9) was least adsorbed (0.85 ng/mm^2) because of its negative charge, and bFGF (17 kDa, pI 10.1), though its molecular weight is 10 times smaller than γ-globulin, was more adsorbed (2.08 ng/mm^2) than albumin because of its positive charge.

The Ti-SPR sensor also enabled us to measure changes in adsorption of polymers to surfaces, like for instance titanium medical devices that are coated with different polymers in order to slowly release drugs and cytokines [37]. Real-time changes in SPR angle shifts were measured when titanium was exposed to PEI, gelatin, and PPAc suspensions, respectively (fig. 8). While PEI and gelatin were rapidly adsorbed onto the titanium surface and resisted removal by washing, PPAc significantly etched the surface due to its low pH (pH; 1.5), but left a thin PPAc layer deposited upon washing [38].

These results indicate that the developed Ti-SPR sensor can accurately measure the time-dependent protein and polymer adsorption process onto the titanium passivation layer.

3.5 SPRI Observation of Cell Response on Titanium Surface

A variant of the sensor enables SPRI-mapping of biological surface processes. Using the SPRI, the cell response onto the polymer-coated titanium array chip could be studied in real-time (fig. 9a and 9b). The response of MC3T3-E1 cells were found to be better to the spots coated with PPAc, titanium, PEI, and gelatin, in this order. Unfortunately, the cell response on the surface contains not only

cell adhesive but also cell reactions [39]. This differential cell adhesion was confirmed by phase-contrast microscopy (fig.9c), which showed that cells adhered onto the PPAc-spot and the gelatin-spot through developed filopodia along with spread cell bodies, while cells on the PEI-spot and Ti-spot clearly showed less filopodia without spread cell bodies. These results indicated that the cell response from SPRI was not correlated with the cell spread area but contained some sort of living-cell actions. Although another measurement method for detecting some cell reaction is needed to be combined, we suppose the study of early cell response to titanium using SPRI could contribute to a better understanding of the early phases of osseointegration of titanium implants, leading to improved osseointegration therapy.

3.6 SPRI Observation of Corrosion Resistance of Titanium Surface

The imaging potential of the Ti-SPR sensor was illustrated in a surface corrosion experiment involving exposure to the HCl/KCl-buffered solution. DDP and ODTCS can immobilize on the surface strongly as a self-assembled monolayer because they have a long alkyl chain and a surface-active head group [40-41], and these immobilized layers were supposed to protect the titanium surface from acid. In figure 10a, the SPRI image of the DDP treated titanium array revealed that the DDP-solution, which is acidic, etched the ODTCS-coated titanium around the DDP-spots. The acid-etching of titanium with HCl leads to the highest corrosion at the titanium-spot, slightly less in the OTDCS-coated surface, while the DDP-spot appeared most resistant to the HCl-acid attack (fig. 10b). This result suggests that these monolayers coated on

titanium surface have a property of corrosion resistance, especially DDP-treated surface.

4. Conclusions

For the titanium medical devices, their surfaces oxidize in air and then have the passivation layer. Our developed Ti-SPR sensor has the similar passivation layer as these devices because the titanium metal layer on the sensor oxides in a similar way. From the results, the Ti-SPR sensor could detect the acid etching, the biomolecule adsorption, the cell reaction, and the corrosion resistance on the titanium surface in real-time assessment.

The Ti-SPR sensor shows a broad applicability to study surface interactions with titanium passivation layer. In Biomaterial Sciences, this instrument most obviously enables investigations of surface chemistry and biomolecular aspects of integration of titanium implants in human bone, especially to gain insight in the earliest processes of protein adsorption and cell attachment, a scientifically important enigma that needs to be clarified in order to further ameliorate implant therapy in dental medicine and orthopedics. This sensor may also prove useful to study interactions of biomolecules and cells with other titanium medical devices used within the human body. In Material Sciences, the process of corrosion could be studied in more depth to further improve the corrosion-resistance of titanium-based machines/equipment used in major marine and aerospace industry. Thus, this innovative high-resolution surface analytical tool could not only be employed to investigate the surface properties of titanium, but also to develop new materials with better surface treatment method

for titanium devices.

Acknowledgements.

This study was supported in part by Grants-in-Aid for Young Scientists (B) (No. 18700428 and 20791467), by Grant-in-Aid for Scientific Research (B) (No. 21390514) for the Ministry of Education, Culture, Sports, Science and Technology, and by a grant from NIH (ROIEB005772). We thank KAKEN PHARMACEUTICAL Co., Ltd. for their supply of bFGF.

[References]

1. Donachie MJ. TITANIUM: A Technical Guide 2nd edition. Ohio: ASM International; 2000. p123-130.
2. Ivasyshyn OM, Aleksandrov AV. Status of the titanium production, research, and applications in the CIS. Mater Sci 2008;44:311-27.
3. Peacock DK. Effective design of high performance corrosion resistant systems for oceanic environments using titanium. Corros Rev 2000;18:295-330.
4. Wake H, Takahashi H, Takimoto T, Takayanagi H, Ozawa K, Kadoi H, et al. Development of an electrochemical antifouling system for seawater cooling pipelines of power plants using titanium. Biotechnol Bioeng 2006;95:468-73.
5. Maciver A, Hinge S, Andersen BJ, Nielsen JB. New trend in desalination for Japanese nuclear power plants, based on multiple effect distillation, with vertical titanium plate falling film heat transfer configuration. Desalination 2005;182:221-8.
6. de Jonge LT, Leeuwenburgh SCG, Wolke JCG, Jansen JA. Organic–Inorganic Surface Modifications for Titanium Implant Surfaces. Pharm Res 2008;25:2357-69.
7. Cilingiroglu M. Long-Term Effects of Novel Biolimus Eluting DEVAX AXXESS Plus Nitinol Self-Expanding Stent in a Porcine Coronary Model. Catheter Cardiovasc Interv 2006;68:271–9.
8. Norlin A, Pan J, Leygraf C. Investigation of Electrochemical Behavior of Stimulation/Sensing Materials for Pacemaker Electrode Applications. I. Pt, Ti, and TiN Coated Electrodes. J Electrochem Soc 2005;152:J7-J15.

9. Meirelles L, Albrektsson T, Kjellin P, Arvidsson A, Franke-Stenport V, Andersson M, et al. Bone reaction to nano hydroxyapatite modified titanium implants placed in a gap-healing model. J Biomed Mater Res Part B 2008;87A:624-31.
10. Ku Y, Chung CP, Jang JH. The effect of the surface modification of titanium using a recombinant fragment of fibronectin and vitronectin on cell behavior. Biomaterials 2005;26:5153–7.
11. Schuler M, Owen GR, Hamilton DW, de Wild M, Textor M, Brunette DM, et al. Biomimetic modification of titanium dental implant model surfaces using the RGDSP-peptide sequence: A cell morphology study. Biomaterials 2006;27:4003-15.
12. Cochran DL, Schenk RK, Lussi A, Higginbottom FL, Buser D. Bone response to unloaded and loaded titanium implants with a sandblasted and acid-etched surface: A histometric study in the canine mandible. J Biomed Mater Res 1998;40:1-11.
13. Langer R, Tirrell DA. Designing materials for biology and medicine. Nature 2004;428:487-92.
14. Kretschmann E. Determination of the optical constants of metals by excitation of surface plasma. Z Phys 1971;241:313–24.
15. Schasfoort RBM, Tudos A. Handbook of Surface Plasmon Resonance. United Kingdom: RSC Publishing; 2008. p15-34.
16. Arima Y, Ishii R, Hirata I, Iwata H. Development of Surface Plasmon Resonance Imaging Apparatus for High-Throughput Study of Protein-Surface Interaction. e-J Surf Sci Nanotech 2006;4;201-7.

17. Anker JN, Hall WP, Lyandres O, Shah NC, Zhao J, Van Duyne RP. Biosensing with plasmonic nanosensors. Nature Mater 2008;7:442-53.
18. Liao HB, Xiao RF, Wang H, Wong KS, Wong GKL. Large third-order optical nonlinearity in Au:TiO_2 composite films measured on a femtosecond time scale. Appl Phys Lett 1998;72:1817-9.
19. Qi ZM, Honma I, Zhou H. Nanoporous leaky waveguide based chemical and biological sensors with broadband spectroscopy. Appl Phys Lett 2007:90:011102.
20. Shinn M, Robertson WM. Surface plasmon-like sensor based on surface electromagnetic waves in a photonic band-gap material. Sensors and Actuators, B: Chemical 2005;B105:360-4.
21. Bernard A, Bosshard HR. Real-time monitoring of antigen-antibody recognition on a metal oxide surface by an optical grating coupler sensor. Eur J Biochem 1995;230:416-23.
22. Plenet JC, Brioude A, Bernstein E, Lequevre F, Dumas J, Mugnier J. Densification of sol-gel TiO_2 very thin films studied by SPR measurements. J Opt Mater 2000;13:411-5.
23. Yao M, Tan OK, Tjin SC, Wolfe JC. Effects of intermediate dielectric films on multilayer surface plasmon resonance behavior. Acta Biomater 2008;4;2016-27.
24. Hirata I, Morimoto Y, Murakami Y, Iwata H, Kitano E, Kitamura H, et al. Study of complement activation on well-defined surfaces using surface plasmon resonance. Colloid Surf B-Biointerfaces 2000;18:285-92.

25. Hirata I, Hioki Y, Toda M, Kitazawa T, Murakami Y, Kitano E, et al. Deposition of complement protein, C3b, on mixed self-assembled monolayers carrying surface hydroxyl and methyl groups studied by surface plasmon resonance. J Biomed Mater Res Part A 2003;66A:669-76.
26. Knoll W. Polymer thin films and interfaces characterized with evanescent light. Makromol Chem 1991;192:2827-56.
27. Azzam RMA, Bashara NM: Ellipsometry and Polarized Light. Amsterdam: North-Holland Personal Library; 1977. p283-363.
28. Choi WS, Kim YM, Combs C, Frohman MA, Beaven MA. Phospholipases D1 and D2 Regulate Different Phases of Exocytosis in Mast Cells. J Immnol 2002;168:5682-9.
29. Bower VE, Bates RG. The pH values of the Clark and Lubs buffer solutions at 25º. J Res Nat Bureau Standard 1955;55:197-200.
30. Dieblod U. The surface science of titanium dioxide. Surf Sci Rep 2003;48;53-229.
31. Lu G, Bernasek SL, Schwartz J. Oxidation of a polycrystalline titanium surface by oxygen and water. Surf Sci 2000;458;80-90.
32. Liu X, Chu PK, Ding C. Surface modification of titanium, titanium alloys, and related materials for biomedical applications. Mater Sci Eng R 2004;47;49-121.
33. Safonova LP, Pryahin AA, Fadeeva JA, Shmukler LE. Viscosities, Refractive Indexes, and Conductivities of Phosphoric Acid in *N,N*-Dimethylformamide + Water Mixtures. J Chem Eng Data 2008;53:1381–6.

34. Kokubo T, KIM HM, Kawashita M, Nakamura T. Bioactive metals: preparation and properties. J Mater Sci-Mater Med 2004;15;99-107.
35. Sul YT, Johansson CB, Kang Y, Jeon DG, Albrektsson T. Bone Reactions to Oxidized Titanium Implants with Electrochemical Anion Sulphuric Acid and Phosphoric Acid Incorporation. Clin Implant Dent Relat Res 2002;4(2);78-87.
36. Parfitt GD. The surface of titanium dioxide. Prog Surf Membrane Sci 1976;11:181-226.
37. Mani G, Johnson DM, Marton D, Feldman MD, Patel D, Ayon AA, et al. Drug delivery from gold and titanium surfaces using self-assembled monolayers. Biomaterials 2008;29:4561–73.
38. Maekawa K, Yoshida Y, Mine A, Fujisawa T, Van Meerbeek B, Suzuki K, et al. Chemical interaction of polyphosphoric acid with titanium and its effect on human bone marrow derived mesenchymal stem cell behavior. J Biomed Mater Res 2007;82A:195–200.
39. Yanase Y, Hiragun T, Kaneko S, Gould HJ, Greaves MW, Hide M. Detection of refractive index changes in individual living cells by means of surface plasmon resonance imaging. Biosens Bioelectron 2010;26;674-81.
40. Spori DM, Venkataraman NV, Tosatti SGP, Durmaz F, Spencer ND, Zürcher S. Influence of Alkyl Chain Length on Phosphate Self-Assembled Monolayers. Langmuir 2007;23(15);8053–60.
41. Liang S, Chen M, Xue Q, Qi Y, Chen J. Site selective micro-patterned rutile TiO2 film through a seed layer deposition. J Colloid Interface Sci 2007; 311(1);194-202.

[Figure legends]

Figure 1

Schematic illustrating the Ti-SPR sensor with coupled prism for SPR. The deposited titanium metal layer is easily oxidized by air and its thickness is changed. The thickness and dielectric constant are indicated for each coated/adsorbed substance (S-LAL10 glass, Cr, Au, Ti, TiO_2, protein, and PBS).

Figure 2

Simulation of SPR spectrum against 0, 20, 40, 60, 80, and 100 % oxidized titanium metal layers by air. Thicknesses of vapor deposited titanium metal layer were (a) 5 nm, (b) 10 nm, and (c) 20 nm.

Figure 3

High-magnification cross-sectional TEM image of the Ti-SPR sensor.

Figure 4

SPR spectrum of the developed Ti-SPR sensor. 5-nm titanium metal layer was deposited on this sensor. The continuous and dotted lines represent the measured and theoretically calculated spectra (titanium; 0.7 nm, titanium dioxide; 7.6 nm), respectively.

Figure 5

Atom fraction of Au (●) and O/Ti (○) ratio on the surface of the Ti-SPR sensor as measured by angle-dependent XPS.

Figure 6

Effect of etching titanium passivation layer with phosphoric acid at different pH, as measured by SPR **(a)** and by QCM **(b)**. The acid solutions were flowed for 20 min and then were washed out with pure water for 19 min.

Figure 7

Time evolution of protein adsorption on titanium passivation layer by SPR. Protein solutions in PBS were 2 μg/ml γ-globulin, 2 μg/ml albumin, and 2 μg/ml bFGF. The protein solutions were flowed for 10 min and then were washed out with PBS for 9 min.

Figure 8

Time evolution of polymer adsorption on titanium passivation layer by SPR. Polymer solutions were 100μg/ml PEI and 100 μg/ml gelatin in PBS, and 1wt% PPAc in water. The polymer solutions were flowed for 10 min and then were washed out with PBS for 9 min.

Figure 9

MC3T3-E1 cell adhesion on the polymer-coated titanium array. **(a)** SPRI image of the array chip after 1-hour incubation with cells. The four spots were titanium (passivation surface), PEI, gelatin, and PPAc as shown in the schematic. **(b)** Real-time assessment of MC3T3-E1 cell response on the polymer-coated

titanium array by SPRI. **(c)** Phase-contrast microscopy of MC3T3-E1 cell attachment.

Figure 10

SPRI imaging of acid-etching of the DDP treated titanium array chip. **(a)** The array chip of four 1-mm spots, of which two spots were titanium (passivation surface, black spots in the schematic), and the two other spots were treated with DDP (red spots in the schematic), amidst the ODTCS-treated titanium (blue surrounding area in the schematic). The SPRI image revealed that the DDP-solution etched the ODTCS-treated titanium near the DDP-spots. **(b)** The whole area, including the four spots and the surrounding area, were exposed to the HCl/KCl buffer (pH=1.5), during which the SPR-reflected light intensity was recorded in real-time using SPRI.

Figure 1

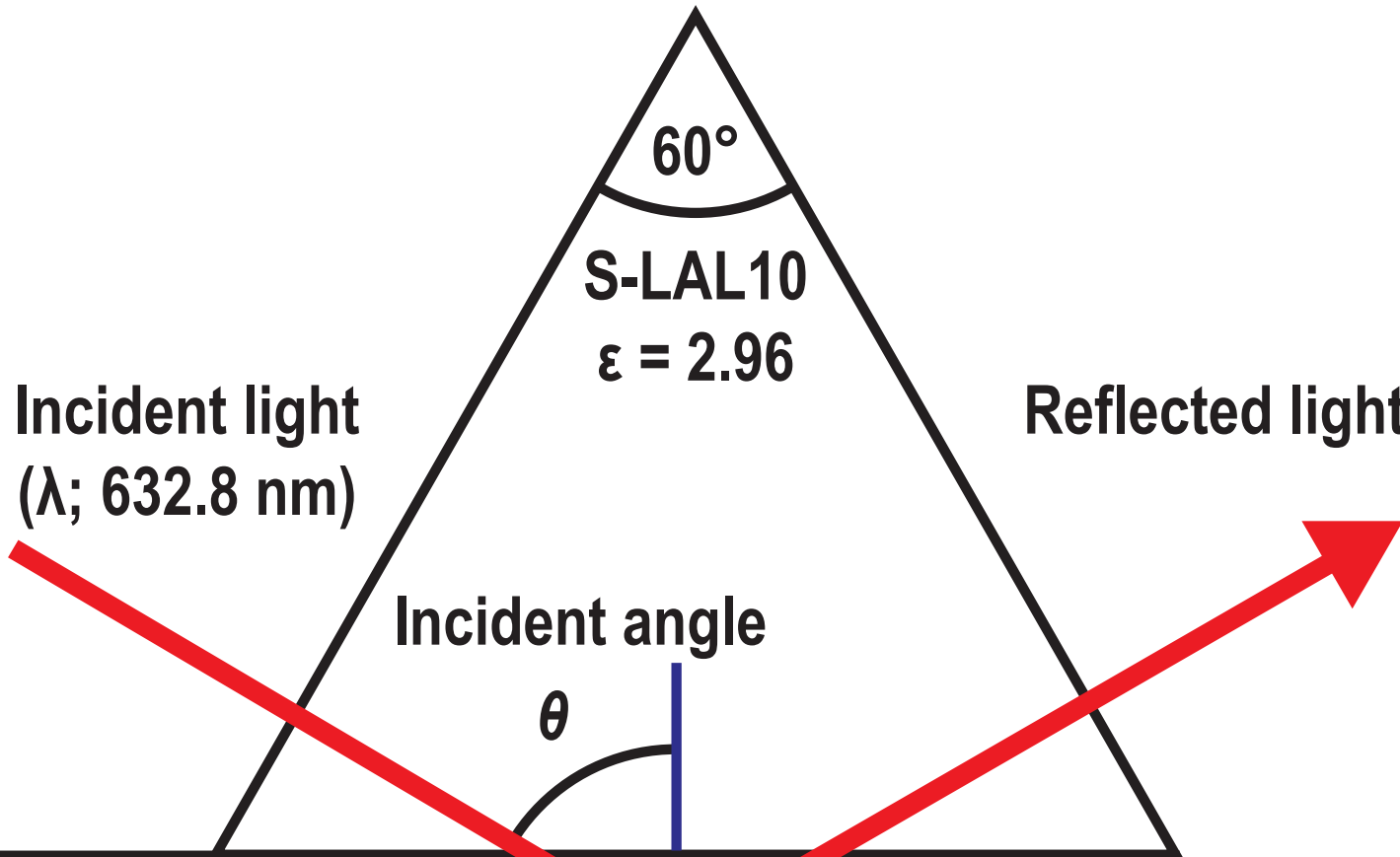

Ti-SPR sensor chip	S-LAL10	
	Cr	ε = -30 + 31i, t = 1 nm
	Au	ε = -12.5 + 1.25i, t = 49 nm
	Ti	ε = -4.30 + 21.1i
	TiO_2	ε = 5.19
Adsorption layer	Protein	ε = 2.10
Medium	PBS	ε = 1.77

Figure 2

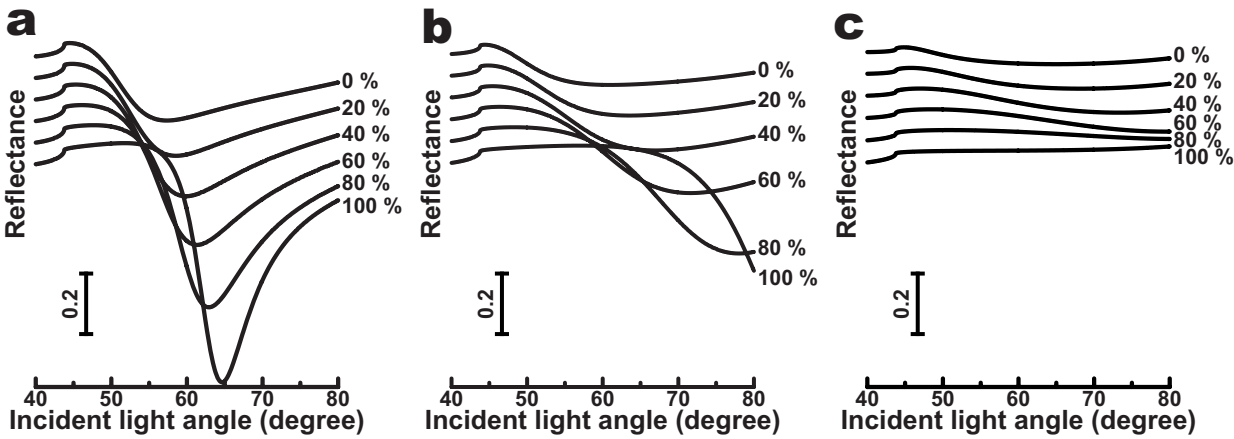
a
b
c
Reflectance
0 %
20 %
40 %
60 %
80 %
100 %
0.2
40
50
60
70
80
Incident light angle (degree)

Figure 3

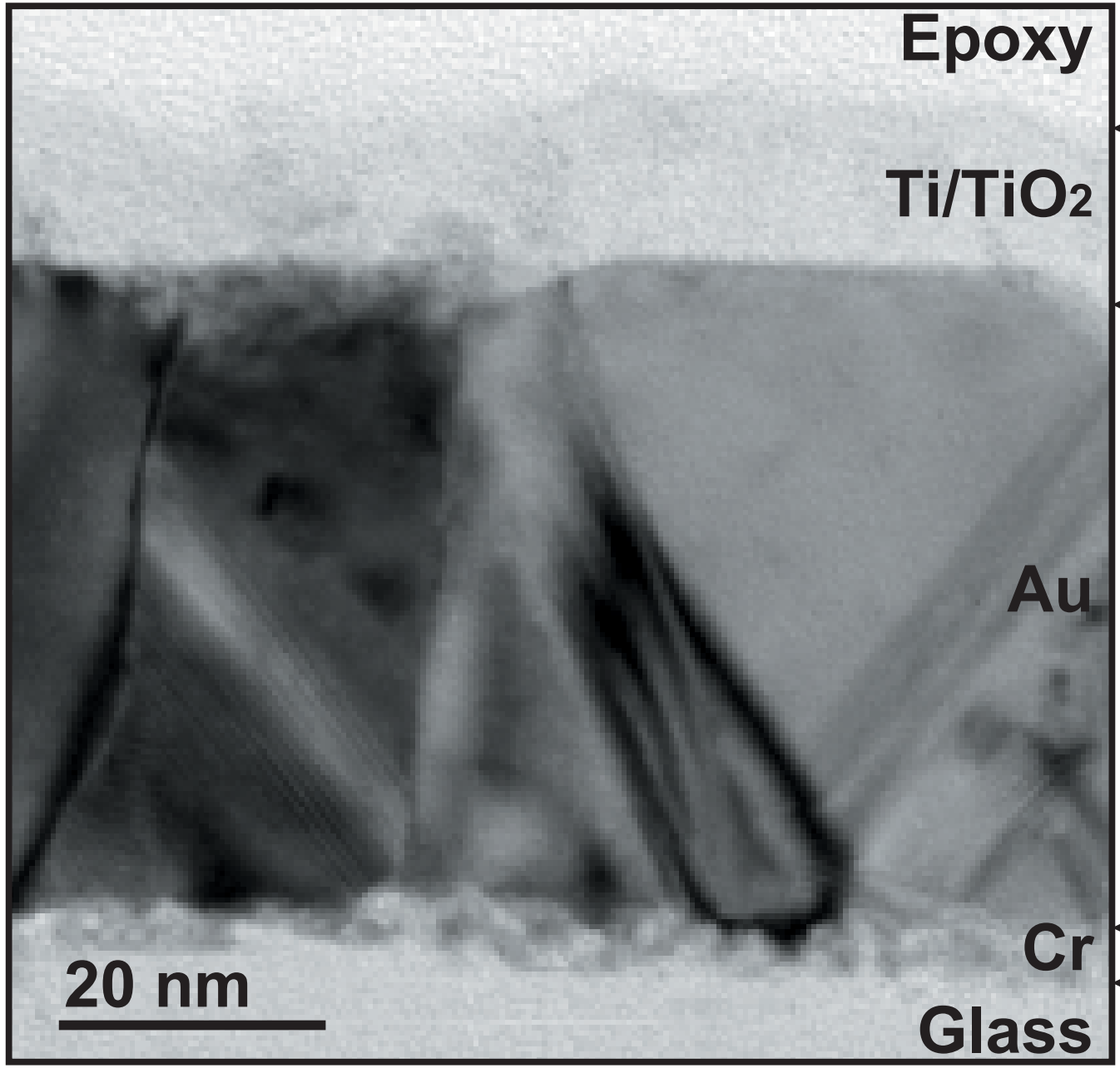

Figure 4

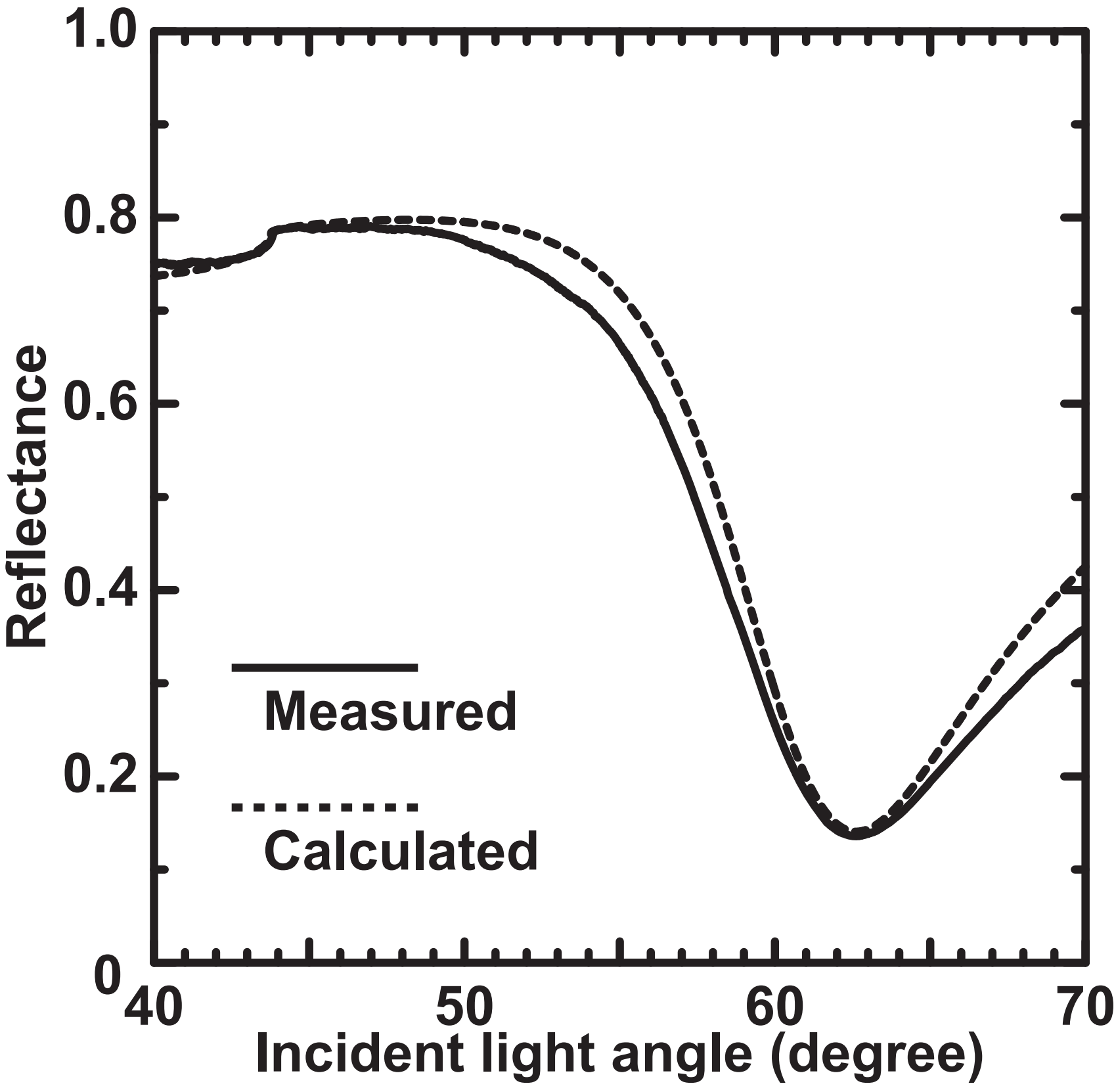
1.0
0.8
0.6
0.4
0.2
0
Reflectance
Measured
Calculated
40
50
60
70
Incident light angle (degree)

Figure 5

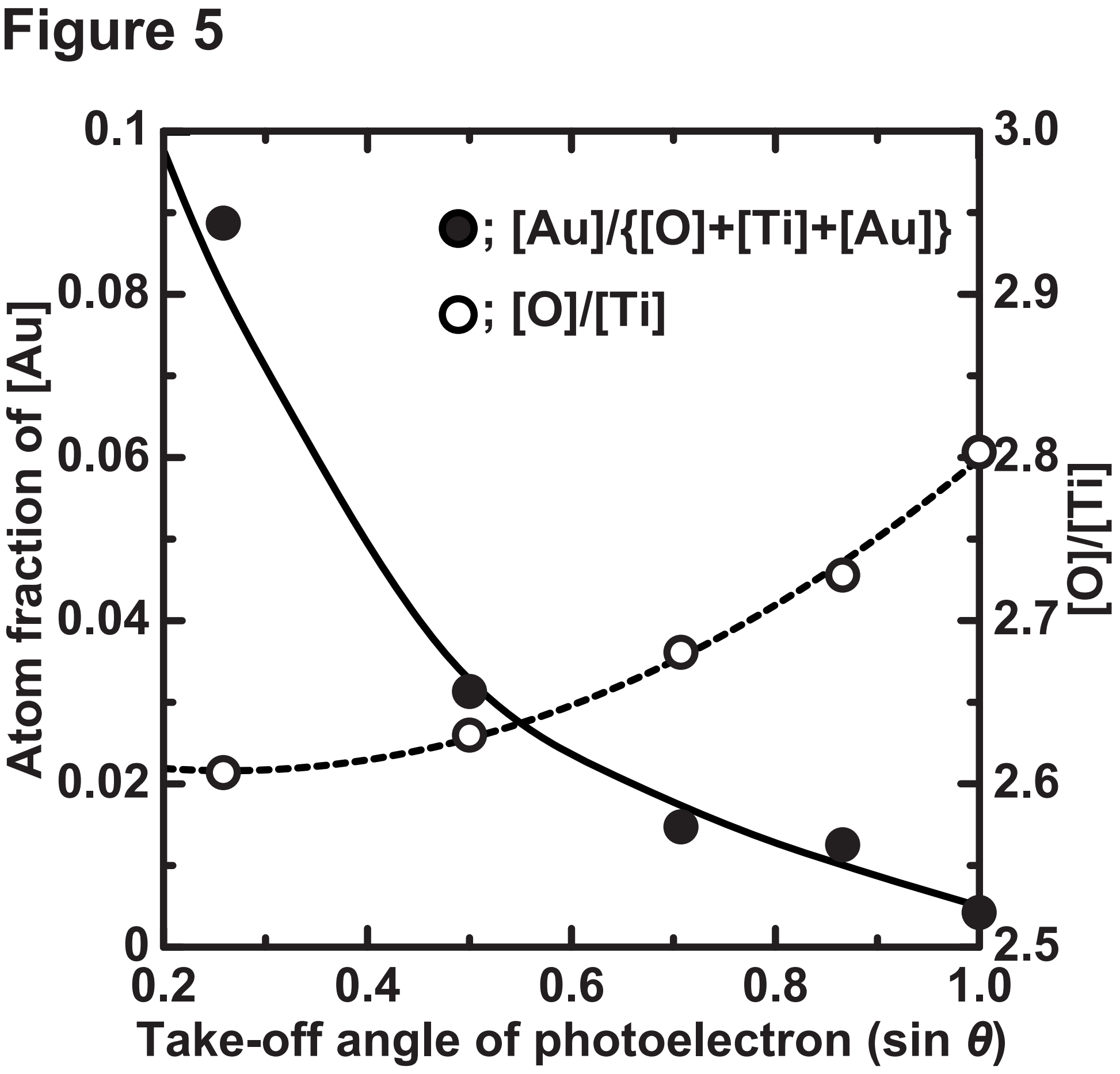
●; [Au]/{[O]+[Ti]+[Au]}
○; [O]/[Ti]
Atom fraction of [Au]
[O]/[Ti]
Take-off angle of photoelectron (sin θ)
0.1
0.08
0.06
0.04
0.02
0
3.0
2.9
2.8
2.7
2.6
2.5
0.2
0.4
0.6
0.8
1.0

Figure 6

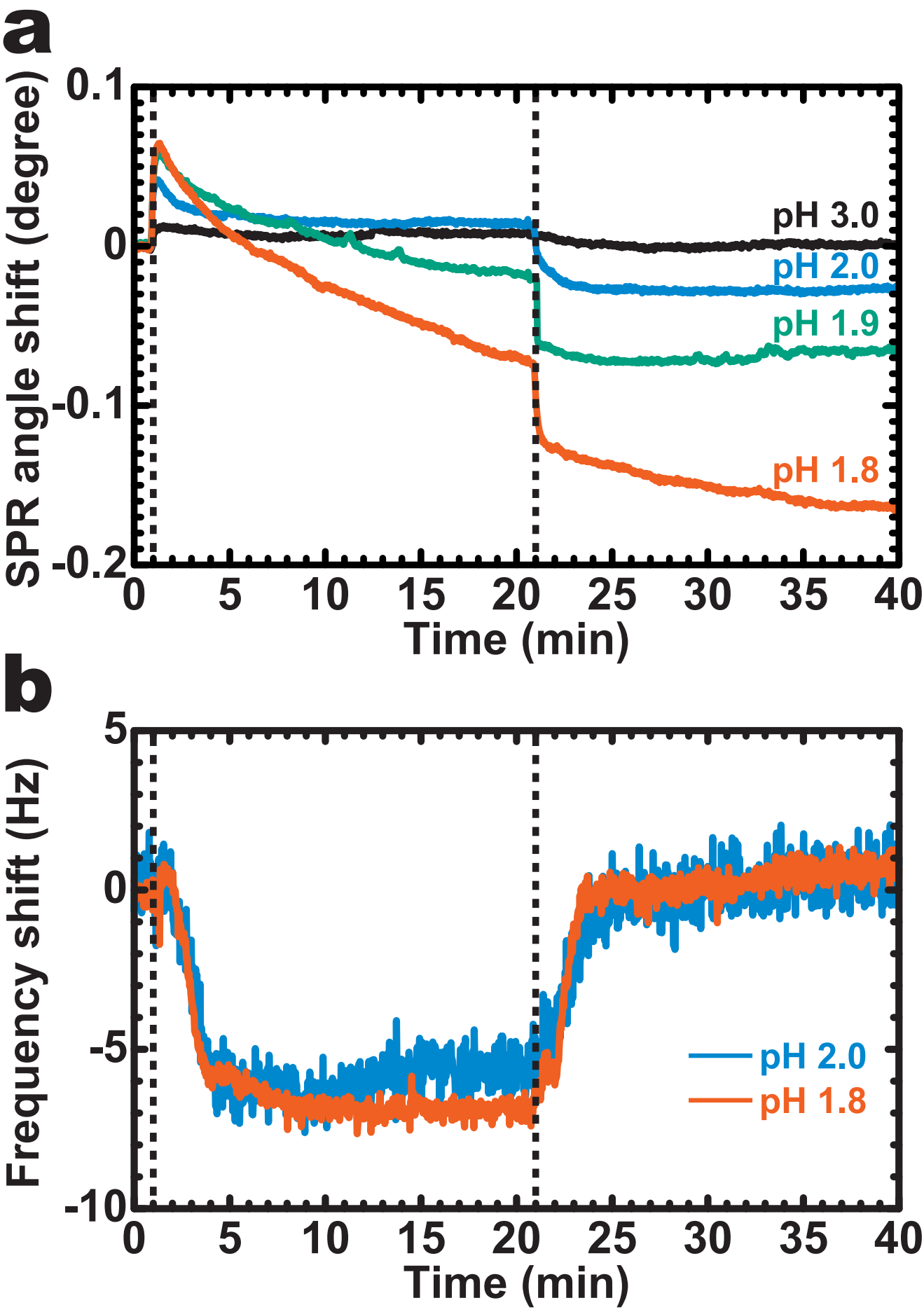
a
SPR angle shift (degree)
0.1
0
-0.1
-0.2
pH 3.0
pH 2.0
pH 1.9
pH 1.8
0
5
10
15
20
25
30
35
40
Time (min)
b
Frequency shift (Hz)
5
0
-5
-10
pH 2.0
pH 1.8
0
5
10
15
20
25
30
35
40
Time (min)

Figure 7

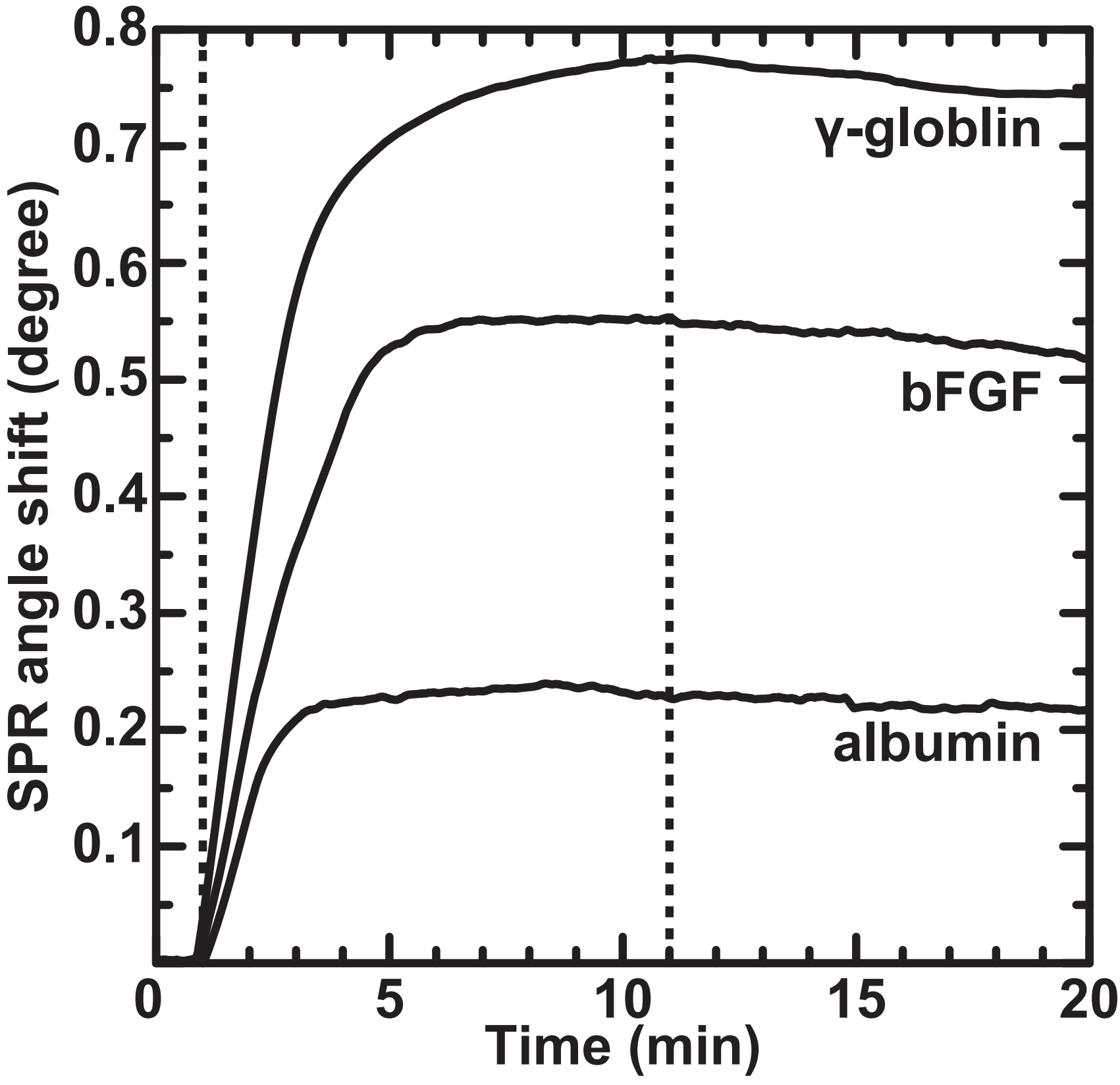
0.8
0.7
0.6
0.5
0.4
0.3
0.2
0.1
SPR angle shift (degree)
γ-globlin
bFGF
albumin
0
5
10
15
20
Time (min)

Figure 8

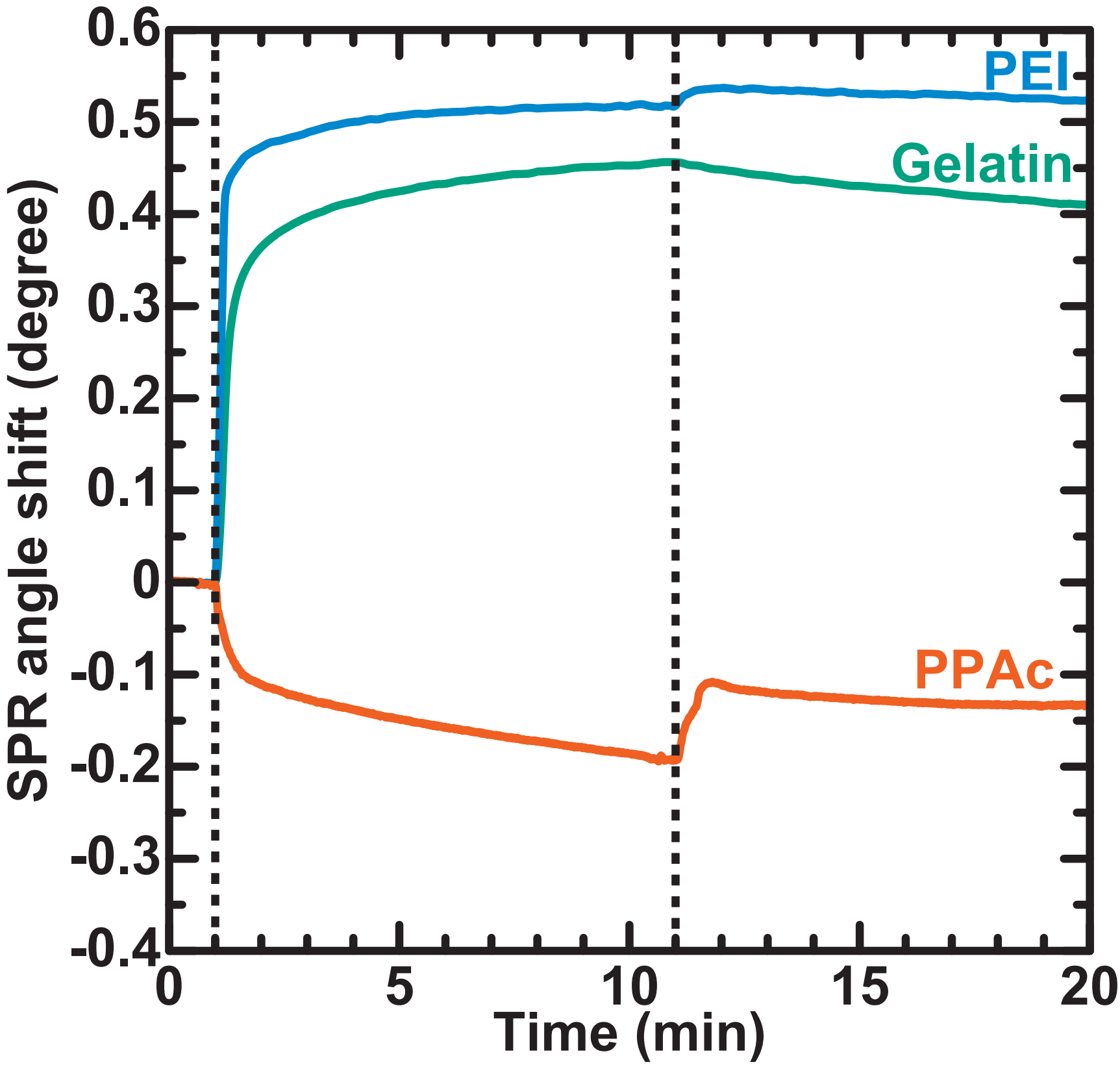
0.6
0.5
0.4
0.3
0.2
0.1
0
-0.1
-0.2
-0.3
-0.4
SPR angle shift (degree)
0
5
10
15
20
Time (min)
PEI
Gelatin
PPAc

Figure 9

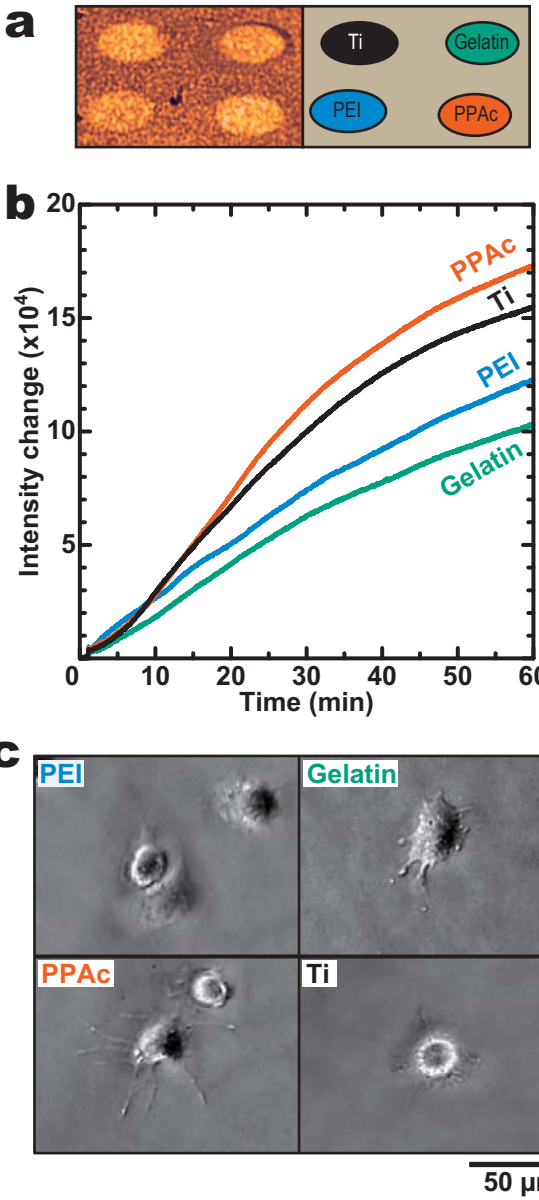
a
Ti
Gelatin
PEI
PPAc
b
Intensity change (x10^4)
Time (min)
PPAc
Ti
PEI
Gelatin
c
PEI
Gelatin
PPAc
Ti
50 μm

Figure 10

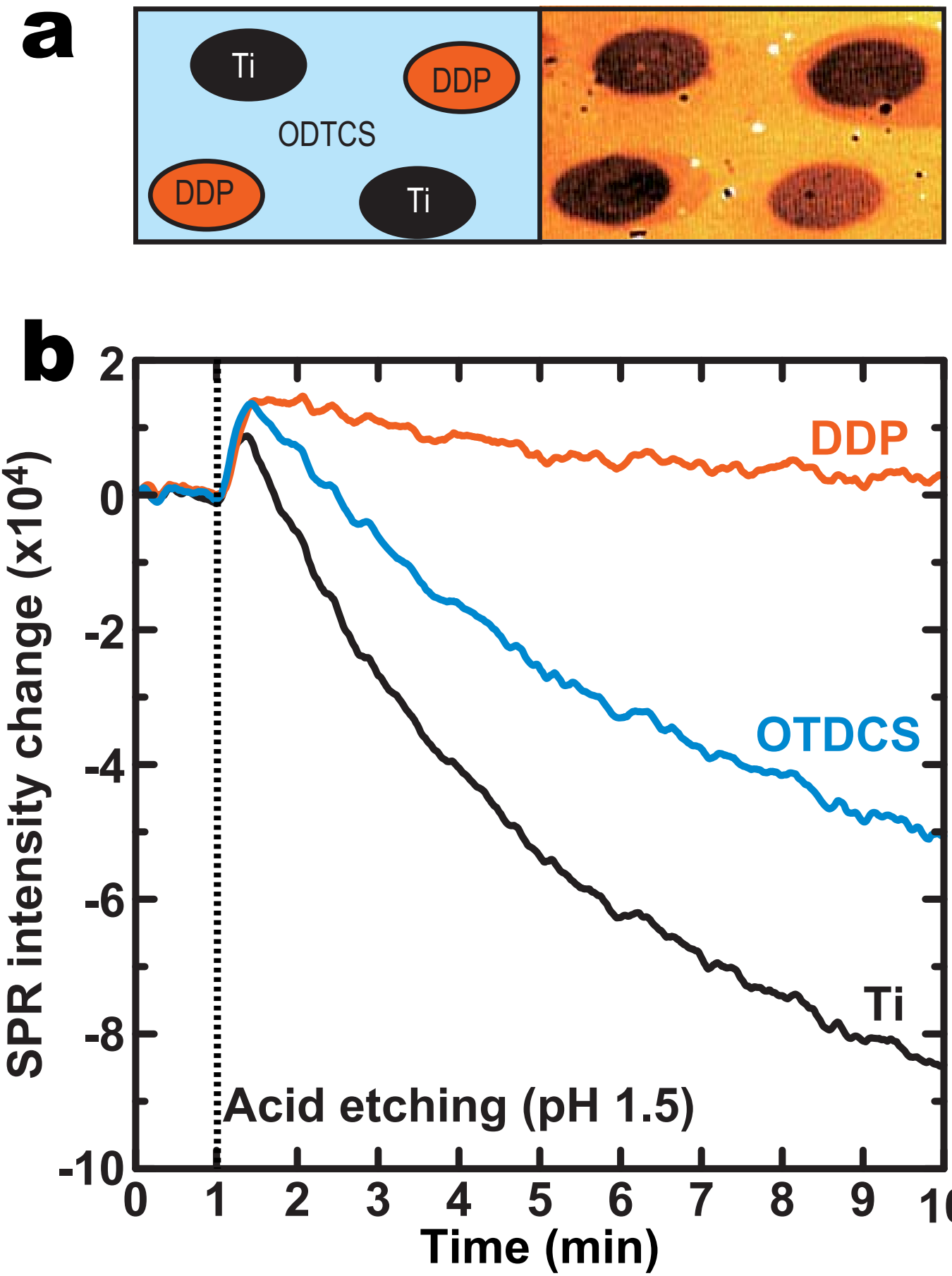
a
Ti
DDP
ODTCS
DDP
Ti
b
SPR intensity change (x10⁴)
2
0
-2
-4
-6
-8
-10
DDP
OTDCS
Ti
Acid etching (pH 1.5)
0
1
2
3
4
5
6
7
8
9
10
Time (min)

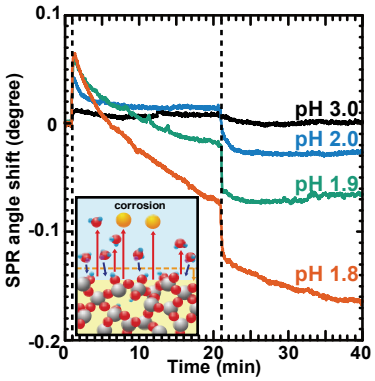

We report for the first time on our development of a titanium passivation layer sensor that makes use of surface plasmon resonance. The deposited titanium metal layer on the sensor was passivated in air, like titanium medical devices. This sensor analyses not only biomolecules interactions but also corrosion of titanium passivation layer exposed to acid in real time and will therefore be very useful to study titanium-corrosion phenomena and biomolecular titanium-surface interactions with application in a broad range of industrial and biomedical fields.